Deep-Target Delivery of Nanosensors with Bacteria-Inspired Coordination

Wei-Kang Hsu, Xiaojun Lin, Mark R. Bell

***Abstract*—This paper studies a nanosensor coordination scheme to effectively deliver nanosensors to deep targets. Deep targets are far away from the main patrolling paths of nanosensors (e.g. blood vessels) and hence the delivery ratio relying on natural diffusion can be very low. Inspired by the communication and motility capability of bacteria, we devise a decentralized coordination strategy so that once the deep target is identified by a small number of nanosensors, they can effectively recruit far-away nanosensors towards the target. Note that since the target is deep, patrolling nanosensors are typically outside the direct communication range of those nanosensors at the location of the target. Therefore, multi-hop communication is required to recruit replenishing agents from the main paths. We demonstrate that the proposed strategy can successfully pull the patrolling nanosensors to the deep target when the model parameters are properly selected. This suggests a potential solution to the open problem in cancer treatments that therapeutic agents are kept away from the central necrotic core of tumors.**

***Index Terms*—Nanosensor coordination, local-decision rule, target detection, swarm robotics**

I. Introduction

Many complex behaviors observed in various animal species are actually formed by simple local interactions. Some notable examples include the navigation of birds [1], swarming of fish [2], and biofilm formation and bioluminescence in bacteria [3], [4]. As the emergence of nanomachines has become promising in recent years [5], [6], communication and coordination among them to achieve more complex objectives has received increased attention [7]–[12]. Indeed, learning from the behaviors of existent species may provide us with insights into designing local decision rules for such nanomachines so that they can collectively perform complex tasks efficiently.

In this work, we study how to design such local decision rules for coordinating nanosensors so that they can be efficiently delivered to deep targets inside the human body, which is an important but challenging problem in applying nanosensors for medicine. An example of a deep target inside the human body is a tumor. Typically, therapeutic agents are carried through blood vessels. They are kept away from necrotic cores of tumors due to leaky vessels. As a result, therapeutic agents are attached mainly to tumor surfaces and hence become less effective. Although certain bacteria have been found to have a tendency to stay around tumor regions and can thus be genetically engineered for targeting treatments [13]–[16], the actual drug delivery rate is still too low to put into clinical practice. It is therefore important to investigate new ways to recruit more therapeutic agents towards deep-target regions.

Some prior work for delivering therapeutic agents to deep targets assumes that the positions of the deep targets are already known. For example, in [17], they constructed a signaling-receiving module to recruit more agents to the target position via nanoparticles. The signaling module, e.g. gold nanorods, are pre-delivered to the tumor site and heated to cause damage to blood vessels in the tumor, as shown in Fig. 1. This will activate the coagulation cascade process and recruit the receiving particles that carry therapeutic cargo. It is shown the proposed system in [17] achieves 40 times higher doses of chemotherapeutics delivered to tumors than non-communicating controls. However, in many cases, since not all deep targets are known when the therapy is delivered, the above methodology does not always apply.

Ideally, we wish the nanosensors to detect deep targets autonomously, e.g., [18] uses bacteria as the tool for sensing unknown target positions. However, since the targets are deep, only a few nanosensors can reach the deep targets. Thus, it is highly desirable that those few agents reaching the target can recruit more nanosensors afterwards. The prior work in nanosensor coordination mainly focuses on recruiting agents that are initially surrounding the targets. In [11], [19], [20], the authors proposed coordination schemes using two chemicals, repellents and attractants, for efficient target tracking and detection. In [12], the authors proposed using two types of nanomachines in a non-diffusion based environment to detect targets. Besides chemical signaling, [10] also proposed the usage of acoustic waves to coordinate nanomachines for detection purposes. However, because of the limited communication capability of nanosensors, the number of nanosensors that can be recruited in the immediate neighborhood is usually low.

In order to increase the effectiveness, it is therefore imperative to be able to use multi-hop communications to recruit nanosensors from far away. An early attempt to devise non-deterministic local rules on nanomachines to recruit nodes to target positions can be found in [7]. They proposed using three different chemicals to attract the nanomachines located near target locations. Some nanomachines differentiate into signal repeater stations when sensing type-1 chemical released from the target location. They then release type-2 chemical to propagate the detected signal. Similarly, some nanomachines that sensed type-2 chemical will release type-3 chemical. Three chemicals are used to avoid the confusion of movements for those nanomachines moving toward the target. Although the strategy can successfully recruit nanomachines in 3-hop distance from the target, its generalization requires n different chemicals to attract nanomachines n hops away for deep-target

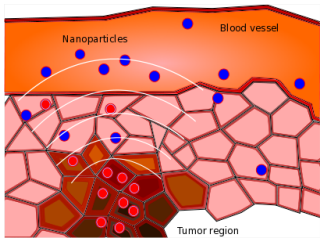

Figure 1: Illustration of signaling particles broadcasting the tumor location to receiving particles, modified from [17].

detection. The requirements of releasing, sensing, and reacting to n different chemicals for the nanomachines lead to high implementation complexity. Therefore, the problem of effectively gathering therapeutic agents towards these abnormal targets using a small number of chemicals remains open.

In this paper, inspired by the coordination mechanism of bacteria, i.e. quorum sensing [4] for population-density detection and chemotaxis [21] for agent navigation, we devise a decentralized rule to gather nanosensors towards deep targets using two chemicals. These targets, typically far from the main patrolling paths of nanosensors, may only be detected by a small number of nanosensors through natural diffusion alone. However, we demonstrate that our proposed strategy allows the few agents reaching the target to successfully recruit faraway patrolling nanosensors via multi-hop signal-cascading paths.

The rest of the paper is organized as follows. In Section II, we describe the system model and the design challenges for node coordination. Section III presents our proposed strategy and justifications. Numerical results are shown in Section IV. Finally, we summarize the contributions and future work in Section V.

II. System Model and Design Challenges

A. Communication Channel Model

In this work, we assume a chemical can be sensed by a nanosensor if its distance to the closest releasing source (which is another nanosensor) is within the effective range of the chemical. Denote R_A and R_B as the effective ranges of the two chemicals *Chm-A* and *Ch-B*, respectively. We use $\delta_j^A(t)$ and $\delta_j^B(t)$ as indicator functions representing that nanosensor j has detected *Chm-A* and *Chm-B* above the sensitivity thresholds at a specific time t. That is, let $\mathcal{N}_A \subset \mathcal{N}$ denote the set of nanosensors releasing *Chm-A*. The rest of the nanosensors $j \in \mathcal{N} \setminus \mathcal{N}_A$ would update $\delta_j^A(t)$ as

$$\delta_j^A(t) = \begin{cases} 1, & \min\limits_{i \in \mathcal{N}_A, i \neq j} ||x_j(t) - x_i(t)|| \leq R_A \\ 0, & \text{otherwise}, \end{cases} \tag{1}$$

where $x_j(t)$ is the location of nanosensor j at time t and $\mathcal{N}$ is the set of all nanosensors. The indicator $\delta_j^B(t)$ is determined similarly. The released chemicals are assumed to diffuse away after a short amount of time. Therefore, constant updates of $\delta_j^a(t)$ and $\delta_j^B(t)$ are necessary.

The above model is suitable for our setting for the following two reasons. First, the nanosensors are sparse in our region of interest. Therefore, the chemical accumulation effect is less crucial, which allows us to model the detection of released chemicals as a function of distances. Second, in our proposed strategy, nanosensors only release guiding chemicals when they are in sparsely populated regions. As a result, the effective range of chemicals is not much affected by chemical accumulations from other nanosensors due to fast decay of chemical concentrations with respect to the distance (see Remark below). The benefit of this model is that it simplifies the analysis for the proposed strategy without loss of generality.

Remark. If each nanosensor releasing an impulse of chemicals is assumed to be a point source, the evolution of concentration can be described by Fick's Law as in [22]

$$C(r,t) = \frac{N}{(4\pi D t)^{3/2}} e^{-r^2/4Dt}, \tag{2}$$

where N is the total number of released molecules and r is the distance from the releasing source. Thus, one can calculate the value of R_A and R_B based on a threshold for detecting the chemical.

B. Navigation of Nanosensors

Each nanosensor is assumed to be capable of sensing two chemicals, *Chm-A* and *Chm-B*, and deciding whether to stay or propel in the direction of high chemical concentration. This is indeed mimicking communication in bacteria communities, in which the collective behavior is synchronized via *quorum sensing*, and the motility of bacteria is based on the *chemotaxis* mechanism [21], which drives them toward higher concentrations of beneficial chemicals, referred to as *attractants*.

Here, *Chm-A* serves the same purpose for attractants, while *Chm-B* serves a similar purpose as *autoinducers* in quorum sensing. In other words, *Chm-A* is the "path indicator" chemical to identify the direction of movement for neighboring nanosensors, while Chm-B is used for nanosensors to sense the population density in their neighborhood. Based on the detected boolean values of $\delta_j^A(t)$ and $\delta_j^B(t)$, each nanosensor takes action $a_j(t) \in \mathcal{A} = \{\text{Monitor, Move, Broadcast, Idle}\}$, based on the decision rule $\rho\left(\delta_j^A(t), \delta_j^B(t)\right)$. Each operation mode in the action set $\mathcal{A}$ is described below:

- *Monitor*: Update $\delta_j^A(t)$ or $\delta_j^B(t)$ based on (1).
- *Broadcast*: Release *Chm-A* molecules at its location.
- *Move*: Propel to the nearest broadcasting neighbor within detectable range.
- *Idle*: Remain idle until next command.

Our goal is therefore to design a local rule ρ such that the collective behavior of the system can recruit nanosensors towards deep targets continuously.

The time is discretized so that at each time step, the position of nanosensors are updated based on their targeted positions and environmental perturbations, which are modeled by additive Gaussian noise. Specifically, the position of nanosensor j is updated according to

$$x_j(t+1) = \hat{x}_j(t+1) + \eta, \tag{3}$$

where $\eta \sim \mathcal{N}(0, \sigma_x^2)$ and the targeted position at time $t+1$, $\hat{x}_j(t+1)$, is given by

$$\hat{x}_j(t+1) = \begin{cases} x_j(t), & a_j(t) \neq \text{Move}, \\ x_{k^*}(t), & a_j(t) = \text{Move}, \end{cases} \tag{4}$$

where k^* is the index of nanosensors which release *Chm-A* and have the shortest distance to $x_j(t)$ within R_A. That is,

$$k^* = \arg\min_{i \in \mathcal{N}_j} ||x_j(t) - x_i(t)||, \tag{5}$$

where

$$\mathcal{N}_j = \{d : d \neq j, ||x_j(t) - x_d(t)|| \leq R_A, \\ a_d(t) = \text{Broadcast}\}. \tag{6}$$

Note that we do not consider the volume occupied by each nanosensor (a.k.a. volume exclusion principle). Also, we assume that nanosensors are synchronized and they have sufficient molecules to release throughput the process.

C. Environment Setup

We assume that the target is located at the center of a square monitoring area $\mathcal{M}$. For ease of demonstration, we also assume the nanosensors are initially distributed uniformly with density λ in the 2D space when the target is found. To model the replenishing source of nanosensors from the main patrolling path, we assume new nanosensors enter the system with a rate of μ from the upper-right corner of $\mathcal{M}$, which then follow the dynamics of (3).

D. Design Challenges

The design of local decision rules to achieve deep-target nanosensor delivery using only two chemicals involves two main challenges:

1) The selection of agents to stay stationary is critical for paths to the deep target being formed autonomously. As we will see later, this can actually be accomplished by quorum sensing via *Chm-B*.
2) Relay nodes for guiding paths should coordinate intelligently (using local information) so that nanosensors can swarm towards the target directions instead of moving in opposite directions. This requires a more careful design as detailed in Section III.

When too many nanosensors move towards the target, fewer of them are left for relaying target location information. The lack of relays could limit the long-term number of nanosensors recruited to the target due to broken guidance paths. On the contrary, if too many nanosensors stay stationary for relay purposes, the number of nanosensors reaching the target will be low as well. Therefore, it is important for the strategy to be robust and balanced between these two objectives.

III. Proposed Strategy

A. Overview

Our proposed strategy is designed based on the following principles. Conceptually, we can categorize nanosensors into two categories based on their intended objectives:

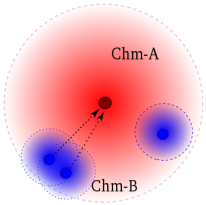

Figure 2: Illustration of "targeting" and "path marker" nanosensors. The center node is a "path marker" in *Broadcast* mode, who wishes to recruit "targeting" nodes. The nodes on the left sense higher concentration of *Chm-B*, and thus some of them will become "targeting" nodes. The nodes on the right sense lower concentration of *Chm-B*, and thus become new "path markers."

1) "Targeting" nanosensors: having the tendency of moving towards target locations so that the target can be treated.
2) "Path marker" nanosensors: broadcasting the target location information to recruit new nanosensors to the targets.

The role of "path marker" or "targeting" nanosensors does not remain unchanged for a given nanosensor. Rather, it is very likely that later coming nanosensors become "path markers" and the previous "path markers" turn into "targeting" agents.

The critical rule to differentiate a nanosensor between the two roles is the neighboring density of nanosensors around it, which is characterized by the concentration of *Chm-B* (see Fig. 2). When the concentration of *Chm-B* is low, a nanosensor is more likely to become a "path marker," which remains in *Broadcast* mode to relay the signal and recruit newcoming nanosensors. A "targeting" nanosensor, on the other hand, operates between *Move* and *Idle* alternatively (Algorithm 1 *line-14* and *line-17*). When no *Chm-A* is sensed, a nanosensor remains in *Idle* mode (*line-17*). The system functions intuitively in that it requires "path marker" nanosensors to remain static to keep the signal-cascading path connected. Those "targeting" nanosensors can then follow the formed cascading path to move closer to the target more effectively, rather than relying on aimless diffusion.

The proposed policy is detailed in Algorithm 1. The release of *Chm-A* at each "path marker" is intelligently scheduled by the proposed policy, such that "targeting" nanosensors move towards the target in multiple hops. P_{Run} (*line 13*, where $u \in [0, 1]$ is a uniformly-distributed random variable) is a designed parameter to trade off nanosensors' converging speed toward the target and the probability that a signal-cascading path to the target stays connected.

B. Broadcast-then-Attract

We refer to the nanosensor reaching the target as at level-0. Nanosensors within the effective range R_A of the target are referred to as at level-1. Similarly, we define nanosensors sensing the cascading signal k hops from the target as at level-k. Further, we denote $s_k(t) \in \mathcal{A}$ as the action that at least one nanosensor in level-k is operating at timeslot t, and $\delta^B_{(l)}(t)$ indicates that nanosensors in level l have sensed *Chm-B* in timeslot t. By default, all the nanosensors have the flag "ToBroadcast" set to *False* initially.

Algorithm 1: Decision rule of each nanosensor j at timeslot t for deep-target delivering

Input: Concentrations of *Chm-A* and *Chm-B*

1 **if** *Reached the target* **then**
2 Broadcast (**Br**) *Chm-A*;
3 return;
4 Update $\delta_j^B(t)$; // neighborhood density flag
5 **if** $\delta_j^B(t) = 0$ and ToBroadcast = True **then**
6 Broadcast (**Br**) *Chm-A*;
7 ToBroadcast $\leftarrow$ True;
8 goto line-17;
9 ToBroadcast $\leftarrow$ False;
10 Update $\delta_j^A(t)$ // sensed *Chm-A* flag
11 **if** $\delta_j^A(t) = 1$ **then**
12 **if** $\delta_j^B(t) = 1$ **then**
13 **if** $u \leq P_{\text{Run}}$ **then**
14 Move to the nearest broadcasting neighbor;
15 **else**
16 ToBroadcast $\leftarrow$ True; // prepare to broadcast
17 Remain *Idle* for the rest of the timeslot;

Notice that the signal-cascading process must initiate at the target location, i.e. at level 0 (*line 1-3*, see also time 0 of Fig. 3). At any given timeslot t, if $s_k(t) = \textit{Broadcast}$ (**Br**), level-$(k+1)$ nanosensors will sense the existence of *Chm-A* and choose three possible actions:

1) If $\delta_{(k+1)}^B(t) = 0$, *line-16* will be executed to set the "ToBroadcast" flag to be *True*. This allows the level-$(k+1)$ nanosensors to prepare broadcasting in the next timeslot so that they can propagate the target information outwardly, as shown by the black nodes between time 0 to time 2 of Fig. 3. This outward propagation continues until it reaches a level l with $\delta_{(l)}^B = 1$.
2) If $\delta_{(k+1)}^B(t) = 1$, nanosensors within level $k+1$ will switch to *Move* with probability P_{Run} and propel to the nearest broadcasting neighbor (by following the largest gradient direction of *Chm-A*). This will lead these moving nanosensors to relocate from level $k+1$ to level k, as shown by the crossed node in time 2 of Fig. 3.
3) If the nanosensors have $\delta_{(k+1)}^B(t) = 1$ but do not enter *line-14*, they will remain *Idle* for the rest of timeslot t (*line-17*), as shown by the white node in level 3 at time 2 of Fig. 3.

Note that one critical requirement for successfully recruiting nanosensors towards the target direction is to guarantee that the moving nodes can only move closer to the targets. In other words, once level-$(k+1)$ nodes move to level-k, the broadcast of *Chm-A* at level k should stop so that these nodes can continue to move to level-$(k-1)$. This requirement is accomplished in Algorithm 1 by allowing broadcast only when a nanosensor is in a sparsely populated region (*line-5*). Thus, if there were nanosensors that moved to the neighborhood

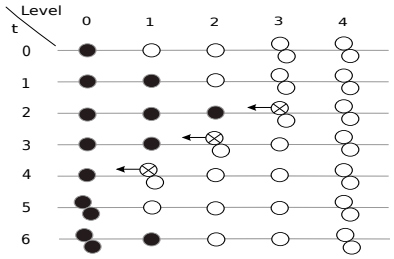

Figure 3: Illustration of system dynamics. The black nodes are broadcasting *Chm-A*, the white nodes are in *Idle*, and the crossed nodes are moving to the nearest broadcasting neighbor. The broadcast initiates at time $t = 0$ at the target location (i.e., level 0).

of broadcast-intended nanosensors (i.e., with ToBroadcast = *True*) in the previous timeslot, the broadcast tendency of the latter nanosensors will be inhibited since $\delta_{(k)}^B(t)$ is updated to 1 (*line-4*). As shown between time 3 and time 4 of Fig. 3, this design allows the nanosensors to be attracted all the way to the target.

In summary, thanks to distributed decisions based on Algorithm 1, the system repeats a very interesting broadcast-then-attract behavior initiating from the location of deep targets. As shown in Fig. 3, *Chm-A* is propagating outwardly via a signal-cascading process until a densely populated nanosensor region is reached. Then, the signal-cascading process is inhibited and alternatively, the system starts to attract available nanosensors until they reach the target. The process is repeated afterwards to recruit more and more faraway nanosensors towards deep targets.

In Section IV, we will show that when all the nodes follow the proposed policy, nanosensors in the main patrolling path can be continuously guided through multi-hop communication towards the deep target.

C. Requirements for R_A and R_B

It is important that R_A and R_B are properly chosen so that the proposed strategy can successfully deliver nanosensors to the deep target continuously. The implementation considerations are discussed below.

1) To maintain the signal-cascading process, the effective range of *Chm-A* should be greater than the distance between each "path marker." This indicates that initially, the range R_A should at least cover another nanosensor from the target location. Therefore, we require R_A to be greater than the expected distance between the two closest nanosensors R_{near}, i.e.

$$R_A > \mathrm{E}[R_{\text{near}}] = \int_0^\infty r\, f(r) dr = \frac{1}{2\sqrt{\lambda}}, \qquad (7)$$

where $f(r) = (2\lambda\pi r)\exp(-\lambda\pi r^2)$, $r > 0$, is the density function of the distance to the nearest nanosensor.
2) The average number of nodes affected by a "path marker" nanosensor should be greater than 1. Otherwise, the cascaded process can be terminated early and fail to

Table I: Simulation parameters

Parameters	Descriptions	Values
R_A	Effective range of *Chm-A*	100 (μm)
R_B	Effective range of *Chm-B*	30 (μm)
$\mathcal{M}$	Monitoring area	1000×1000 (μm^2)
λ	Local density of agents in $\mathcal{M}$	3×10^{-4} ($1/\mu$m^2)
μ	Rate of agents entering the system	1 (1/timeslot)
P_{Run}	Probability of movement when both δ_j^A and δ_j^B equal to 1	0.1
σ_x	Standard deviation of the agent location disturbances	2 (μm)

propagate outward from the target location. This leads us to the requirement of

$$\lambda \pi (R_A^2 - R_B^2) > 1. \tag{8}$$

IV. Numerical Results

A. Configurations

In our simulations, we set the default parameters as shown in Table I unless otherwise stated. The release of chemicals is assumed to stay effective for one timeslot, afterwards it is lost due to chemical diffusion. Note that we do not assume $\mathcal{M}$ to have a closed boundary. That is, nanosensors can move out of boundary due to moving disturbances. As explained in section II.C, the replenishing source of nanosensors is assumed to provide new nanosensors with a rate, $\mu = 1$, located at the upper-right corner of $\mathcal{M}$. The nodes experience Brownian motion-like trajectory unless sensing the recruiting chemical *Chm-A*.

B. Results

In Fig. 4, the time snapshots of the system simulation are shown to demonstrate the signal-cascading process. Initially, *Chm-A* is released at the target location since only one nanosensor finds the target. Later on, we can observe a growing number of nanosensors moving toward the target, while "path markers" are continuously broadcasting the target location to recruit greater numbers of nanosensors from farther distances.

In Fig. 5, we show the number of nanosensors reaching the target as time elapses. With larger P_{Run}, we see initially a larger amount of nanosensors converging to the target. However, the signal-cascading path is more fragile and subject to disconnection due to a higher tendency of movement for nanosensors, leading to fewer agents capable of reaching the target eventually. In contrast, the system with smaller P_{Run} has an initially smaller converging speed of nanosensors toward the target. However, since the cascading process can be kept intact with higher probability, agents reach the target with a more constant rate, which eventually leads to better target detection than that of the larger P_{Run}.

For the performance metric, we define the steady-state arrival rate of nanosensors π at the target as

$$\pi = \frac{N(t_f) - N(t_1)}{t_f - t_1}, \tag{9}$$

where $N(t)$ is the number of nanosensors reaching the target at time t, t_f is the final observation time and t_1 is the time that the system leaves the transient state. Based on Fig. 5, we chose $t_1 = 100$, indicating that the nanosensors recruited within distance R_A from the target are excluded from the calculation.

Fig. 6 and Fig. 7 show the change of rate π with different values of R_A and R_B. Intuitively, a larger R_A leads to a larger recruitment region, and therefore the rate of gathered nanosensors increases as long as the cascading paths cover the replenishing source. On the contrary, there exists an optimal R_B to maximize the rate of reaching nanosensors for a given R_A. If R_B is too small, then too many nanosensors stay static serving as "path indicators." If R_B is too large, fewer nanosensors can be recruited since the range difference, $R_A - R_B$, becomes small. Hence, there is a best R_B that trade off between the two. Observe that when the model parameters are selected properly, system performance can be enhanced significantly compared to solely relying on natural diffusion.

V. Conclusion

We studied a nanosensor coordination strategy that can recruit nanosensors from the mainstreams (e.g. blood vessels) towards deep-target locations using only two chemicals. We demonstrated that nanosensors can autonomously form "path markers" and guide new nanosensors via a multi-hop signal-cascading path. Bacteria-based gene therapy and drug delivery can benefit from this result in many scenarios where delivering therapeutic cargo into the core of tumors is necessary.

In future work, we will study how to find P_{Run} to optimize the nanosensors' converging speeds to the target and to minimize the probability of disconnecting the signal-cascading paths. It is also important to improve the error resilience of the strategy and to generalize it to accommodate settings where chemicals released by different nanosensors interfere with each other.

References

[1] M. Nagy, Z. Ákos, D. Biro, and T. Vicsek, "Hierarchical group dynamics in pigeon flocks," *Nature*, vol. 464, no. 7290, pp. 890–893, 2010.

[2] J. K. Parrish, S. V. Viscido, and D. Grunbaum, "Self-organized fish schools: an examination of emergent properties," *The biological bulletin*, vol. 202, no. 3, pp. 296–305, 2002.

[3] K. Lemon, A. Earl, H. Vlamakis, C. Aguilar, and R. Kolter, "Biofilm development with an emphasis on bacillus subtilis," in *Bacterial Biofilms*. Springer, 2008, pp. 1–16.

[4] K. H. Nealson, T. Platt, and J. W. Hastings, "Cellular control of the synthesis and activity of the bacterial luminescent system," *Journal of bacteriology*, vol. 104, no. 1, pp. 313–322, 1970.

[5] I. F. Akyildiz, F. Brunetti, and C. Blázquez, "Nanonetworks: A new communication paradigm," *Computer Networks*, vol. 52, no. 12, pp. 2260–2279, 2008.

[6] C. Selin, "Expectations and the emergence of nanotechnology," *Science, Technology & Human Values*, vol. 32, no. 2, pp. 196–220, 2007.

[7] M. A. Lewis and G. A. Bekey, "The behavioral self-organization of nanorobots using local rules." in *IROS*, 1992, pp. 1333–1338.

[8] A. Shklarsh, G. Ariel, E. Schneidman, and E. Ben-Jacob, "Smart swarms of bacteria-inspired agents with performance adaptable interactions," *PLoS Comput Biol*, vol. 7, no. 9, p. e1002177, 2011.

[9] W.-K. Hsu, M. R. Bell, and X. Lin, "Carrier allocation in mobile bacteria networks," in *Signals, Systems and Computers, 2015 49th Asilomar Conference on*. IEEE, 2015, pp. 59–63.

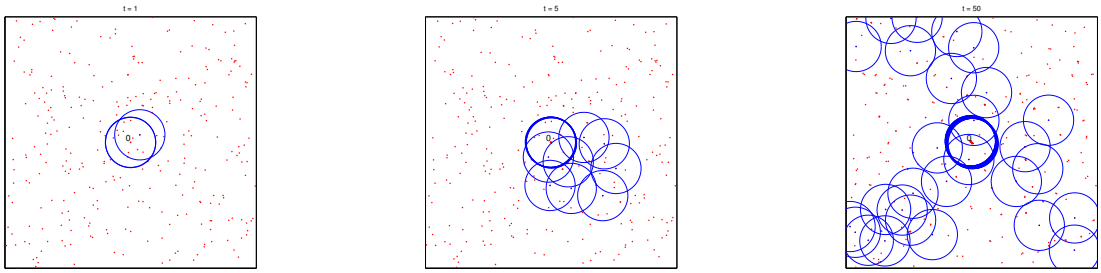

Figure 4: Shows the snapshots of nanosensors gathering toward the target, while constructing "path markers" along multiple paths to recruit later coming nodes. The images are sampled at time $t = 1, 5, 50$, from left to right. The target is located at the center of the monitoring area. The circles represent the effective ranges of *Chm-A* due to nanosensors in *Broadcast* mode.

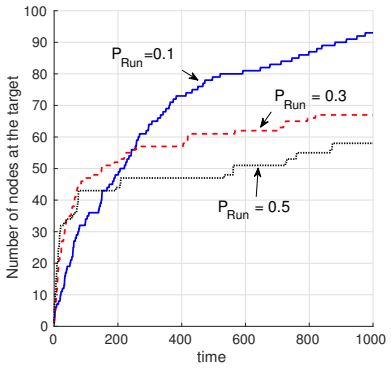

Figure 5: Shows the effect of P_{Run} on the gathering number of nanosensors towards the target. The unit of time is timeslot. Smaller P_{Run} leads to more durable signal-cascading path and ends up recruiting more nanosensors.

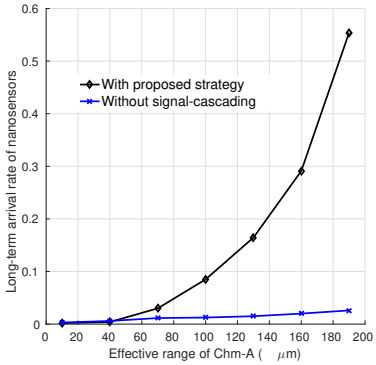

Figure 6: The rate of nanosensors reaching the target increases with increasing values of R_A under the proposed policy.

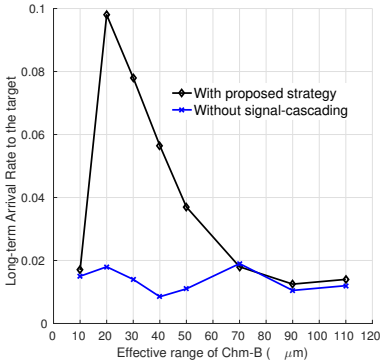

Figure 7: The rate of nanosensors reaching the target for various values of R_B with fixed R_A = 100 (μm).

[10] V. Loscri and A. Vegni, "An acoustic communication technique of nanorobot swarms for nanomedicine applications," 2015.

[11] S. Iwasaki, J. Yang, A. O. Abraham, J. L. Hagad, T. Obuchi, and T. Nakano, "Modeling multi-target detection and gravitation by intelligent self-organizing bioparticles," in *Global Communications Conference (GLOBECOM), 2016 IEEE*. IEEE, 2016, pp. 1–6.

[12] T. Nakano, S. Kobayashi, T. Koujin, C.-H. Chan, Y.-H. Hsu, Y. Okaie, T. Obuchi, T. Hara, Y. Hiraoka, and T. Haraguchi, "Leader-follower based target detection model for mobile molecular communication networks," in *Proceedings of the IEEE International workshop on Signal Processing advances in Wireless Communications (SPAWC)*, 2016.

[13] S. J. Park, S.-H. Park, S. Cho, D.-M. Kim, Y. Lee, S. Y. Ko, Y. Hong, H. E. Choy, J.-J. Min, J.-O. Park *et al.*, "New paradigm for tumor theranostic methodology using bacteria-based microrobot," *Scientific reports*, vol. 3, p. 3394, 2013.

[14] C.-H. Luo, C.-T. Huang, C.-H. Su, and C.-S. Yeh, "Bacteria-mediated hypoxia-specific delivery of nanoparticles for tumors imaging and therapy," *Nano letters*, vol. 16, no. 6, pp. 3493–3499, 2016.

[15] C. Piñero-Lambea, D. Ruano-Gallego, and L. Á. Fernández, "Engineered bacteria as therapeutic agents," *Current opinion in biotechnology*, vol. 35, pp. 94–102, 2015.

[16] D. Akin, J. Sturgis, K. Ragheb, D. Sherman, K. Burkholder, J. P. Robinson, A. K. Bhunia, S. Mohammed, and R. Bashir, "Bacteria-mediated delivery of nanoparticles and cargo into cells," *Nature nanotechnology*, vol. 2, no. 7, pp. 441–449, 2007.

[17] G. Von Maltzahn, J.-H. Park, K. Y. Lin, N. Singh, C. Schwöppe, R. Mesters, W. E. Berdel, E. Ruoslahti, M. J. Sailor, and S. N. Bhatia, "Nanoparticles that communicate in vivo to amplify tumour targeting," *Nature materials*, vol. 10, no. 7, pp. 545–552, 2011.

[18] G. Wei, P. Bogdan, and R. Marculescu, "Bumpy rides: Modeling the dynamics of chemotactic interacting bacteria," *IEEE Journal on Selected Areas in Communications*, vol. 31, no. 12, pp. 879–890, 2013.

[19] Y. Okaie, T. Nakano, T. Hara, and S. Nishio, "Autonomous mobile bionanosensor networks for target tracking: A two-dimensional model," *Nano Communication Networks*, vol. 5, no. 3, pp. 63–71, 2014.

[20] Y. Okaie, T. Nakano, T. Hara, T. Obuchi, K. Hosoda, Y. Hiraoka, and S. Nishio, "Cooperative target tracking by a mobile bionanosensor network," *NanoBioscience, IEEE Transactions on*, vol. 13, no. 3, pp. 267–277, 2014.

[21] J. Adler, "Chemotaxis in bacteria," *Science*, vol. 153, no. 3737, pp. 708–716, 1966.

[22] H. C. Berg, *Random walks in biology*. Princeton University Press, 1993.